

SUPPORTING INFORMATION

M. Arvani, K. Virkki, F. Abou-Chahine, A. Efimov, N. V. Tkachenko and D. Lupo

Synthesis of Phthalocyanine (Pc):

3,3'-[(9(10),15(16),23(24)-Tri-*tert*-butyl-29*H*,31*H*-phthalocyanine-1,4-diyl)bis(oxy)]dipropan-1-ol was prepared according to Ref [1].

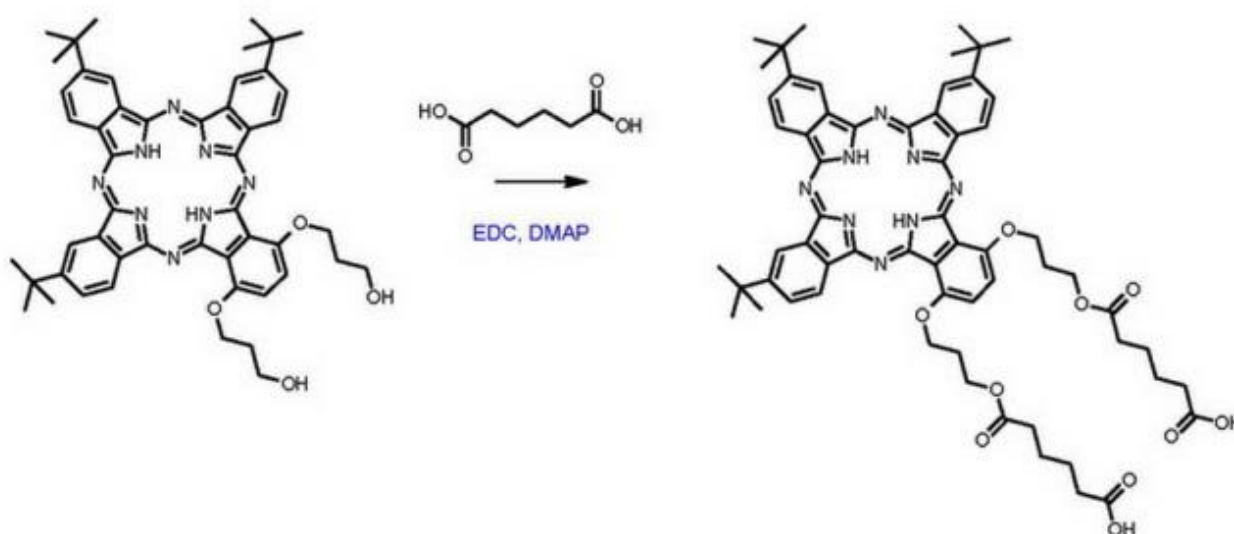


Figure S1. The structure of carboxylic acid functionalized phthalocyanine.

Synthesis of 6,6'-[(9(10),15(16),23(24)-tri-*tert*-butyl-29*H*,31*H*-phthalocyanine-1,4-diyl)bis(oxypropane-3,1-diyloxy)]bis(6-oxohexanoic acid): 3,3'-[(9(10),15(16),23(24)-Tri-*tert*-butyl-29*H*,31*H*-phthalocyanine-1,4-diyl)bis(oxy)]dipropan-1-ol (20 mg, 0.024 mmol), adipic acid (28 mg, 0.192 mmol) and DMAP (23mg, 0.192 mmol) were dissolved in 10 ml of dry DCM. N-(3-Dimethylaminopropyl)-N'-ethylcarbodiimide hydrochloride (36 mg, 0.192 mmol) was added, and the reaction mixture was stirred at r.t. for 14 h.

The solution was washed with water (2×20 ml), evaporated to dryness. TLC analysis (Silica 60 plates, eluent chloroform/ethanol 9/1) revealed a complex mixture of products. Multiple minor spots were found having R_f 0.7-0.5, and a major product with R_f 0.3. The spot was identified with HRMS as the target compound.

Purification was done on a Silica 100 column by gradient elution with a) chloroform; b) chloroform ethanol 10/1; c) chloroform/ethanol/acetic acid 20/1/0.1. With the latter system the target compound was isolated as a green band, yielding after evaporation 6 mg (27%) of the substance as a dark blue solid. $^1\text{H NMR}$ (δ ppm, $\text{CDCl}_3+\text{CD}_3\text{OD}$): 9.52-8.70 (m, 6H, phthalo-H), 8.29-7.97 (m, 3H, phthalo-H), 7.11-6.64 (m, 2H, phthalo-H), 4.89-4.16 (m, 8H, oxo-H), 2.49-2.05 (m, 8H, alfa-carboxy-H), 1.99-1.02 (m, 43H, tert-butyl-H, alkyl-H), -1.34- -1.94 (m, 2H, N-H). ESI-TOF m/z: calculated for $\text{C}_{62}\text{H}_{70}\text{N}_8\text{O}_{10}$ ($\text{M}+\text{H}$) $^+$, 1087.5293, 1088.5325, 1089.5355; found 1087.5344, 1088.5382, 1089.5435.

Differential pulse voltammetry (DPV) measurements:

Samples of Pc in CHCl_3 were analyzed to determine the highest occupied molecular orbital (HOMO) by Differential pulse voltammetry method.

Pc:

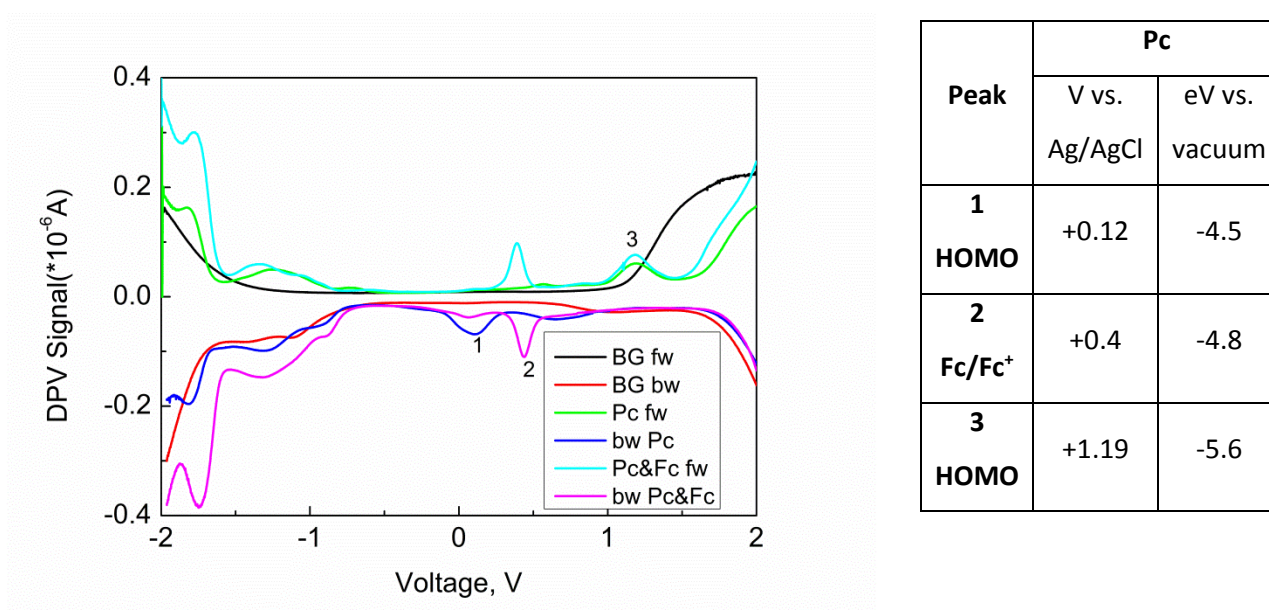
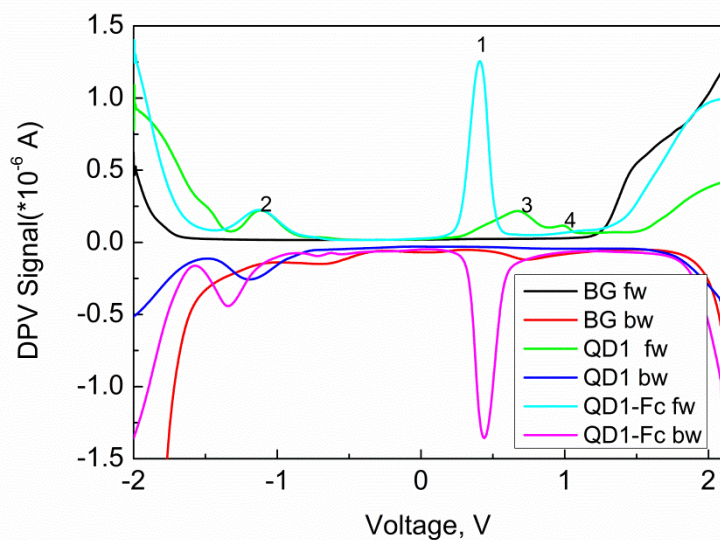


Figure S2. Differential pulse voltammogram of Pc: Background scans in forward (BG fw) and backward (BG bw) direction scans, Pc forward (Pc fw) and backward (Pc bw) and Pc plus ferrocene (Fc) in forward and backward (Pc&Fc), The right shows the reduction and oxidation potentials obtained by the DPV scans for Pc versus Fc/Fc $^+$ and vacuum level.

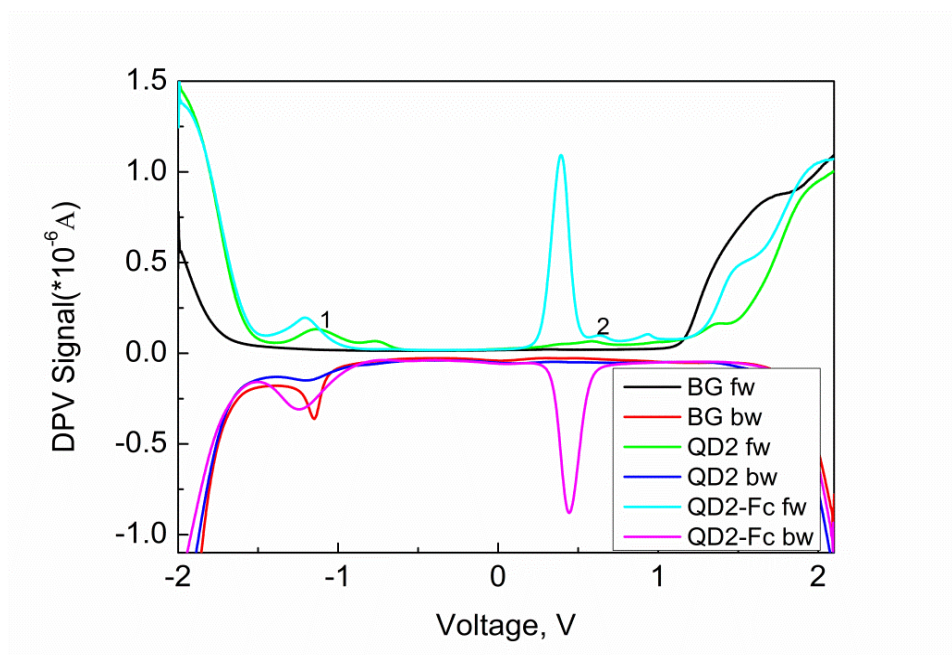
QD1:



Peak	QD1	
	V vs. Ag/AgCl	eV vs. vacuum
1 Fc/Fc ⁺	+0.4	-4.80
2 HOMO	+0.6	-5.06
3 HOMO- 1	+0.97	-5.37

Figure S3. Differential Pulse Voltammogram of QD1: Background scans in forward (BG fw) and backward (BG bw) direction scan, QD1 in forward (QD1 fw) and backward (QD1 bw) direction and QD1 plus Fc in forward (QD1 & Fc fw) and backward (QD1 & Fc bw) direction. The right shows the reduction and oxidation potentials obtained by the DPV scans for QD1 versus Fc/Fc⁺ and vacuum level.

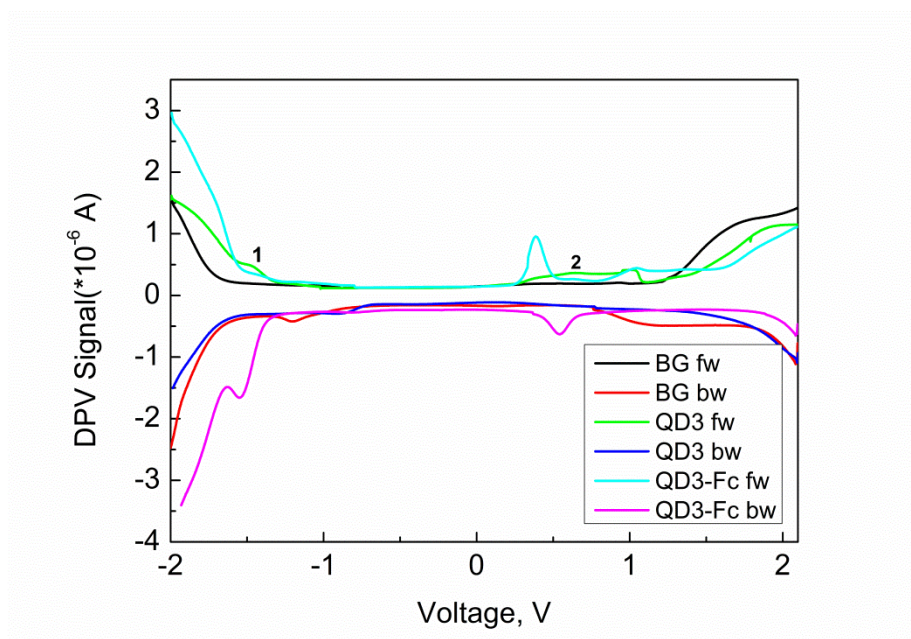
QD2:



Peak	QD2	
	V vs. Ag/AgCl	eV vs. vacuum
LUMO	-1.13	-3.28
HOMO	+0.57	-4.98
Fc/Fc ⁺	0.39	-4.80

Figure S4. Differential Pulse Voltammogram of QD2: Background scans in forward (BG fw) and backward (BG bw) direction scan, QD2 in forward (QD2 fw) and backward (QD2 bw) direction and QD2 plus Fc in forward (QD2 & Fc fw) and backward (QD2 & Fc bw) direction. The right shows the reduction and oxidation potentials obtained by the DPV scans for QD2 versus Fc/Fc⁺ and vacuum level.

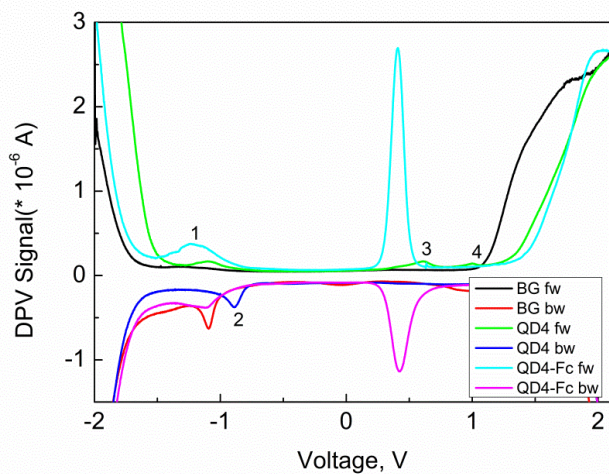
QD3:



Peak	QD3	
	V vs. Ag/AgCl	eV vs. vacuum
LUMO	-1.48	-3.49
HOMO	0.66	-5.08
Fc/Fc ⁺	+0.38	-4.8

Figure S5. Differential Pulse Voltammogram of QD3: Background scans in forward (BG fw) and backward (BG bw) direction scan, QD3 in forward (QD3 fw) and backward (QD3 bw) direction and QD3 plus Fc in forward (QD3 & Fc fw) and backward (QD3 & Fc bw) direction. The right shows the reduction and oxidation potentials obtained by the DPV scans for QD3 versus Fc/Fc⁺ and vacuum level.

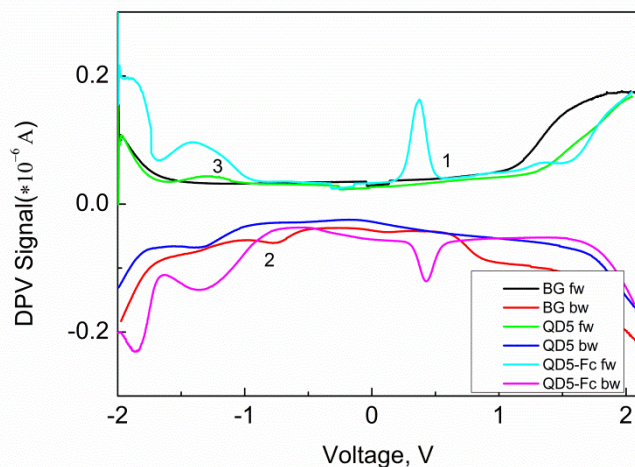
QD4:



Peak	QD4	
	V vs. Ag/AgCl	eV vs. vacuum
LUMO	-0.88	-3.52
LUMO+1	-1.1	-3.3
HOMO	+0.6	-5
HOMO-1	+1	-5.4
Fc/Fc ⁺	0.4	-4.80

Figure S6. Differential Pulse Voltammogram of QD4: Background scans in forward (BG fw) and backward (BG bw) direction scan, QD4 in forward (QD4 fw) and backward (QD4 bw) direction and QD4 plus Fc in forward (QD4 & Fc fw) and backward (QD4 & Fc bw) direction. The right shows the reduction and oxidation potentials obtained by the DPV scans for QD4 versus Fc/Fc⁺ and vacuum level.

QD5:



Peak	QD5	
	V vs. Ag/AgCl	eV vs. vacuum
LUMO (peak1)	+0.5	-4.9
Peak 2	-0.97	-3.43
Peak 3	-1.25	-3.15
Fc/Fc ⁺	+0.4	-4.8

Figure S7. Differential Pulse Voltammogram of QD5: Background scans in forward (BG fw) and backward (BG bw) direction scan, QD5 in forward (QD5 fw) and backward (QD5 bw) direction and QD5 plus Fc in forward (QD5 & Fc fw) and backward (QD5 & Fc bw) direction. The right shows the reduction and oxidation potentials obtained by the DPV scans for QD5 versus Fc/Fc⁺ and vacuum level.

Absorption spectra of QDs:

Absorption spectra of samples of QDs dissolved in CHCl_3 with a pathlength of 1 cm, the concentration of QDs are $2 \mu\text{M}$.

QD1:

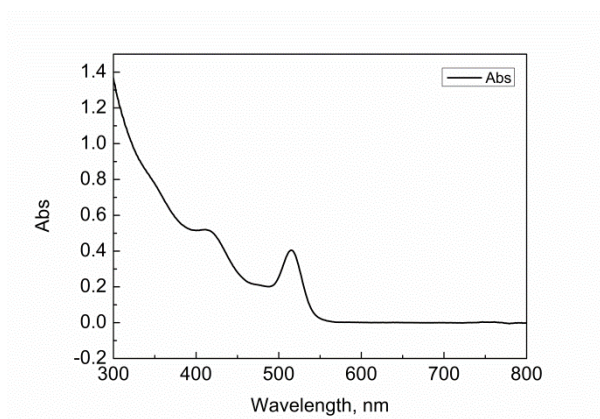


Figure S8. Absorption spectrum of QD1 in CHCl_3 .

QD2:

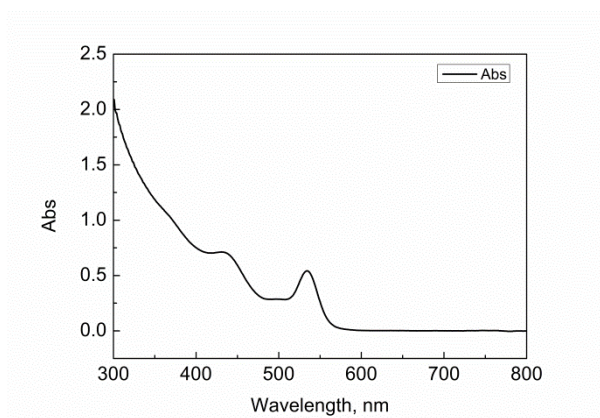


Figure S9. Absorption spectrum of QD2 in CHCl_3 .

QD3:

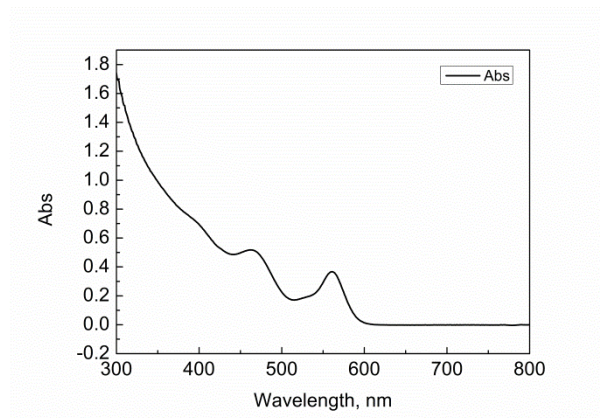


Figure S10. Absorption spectrum of QD3 in CHCl_3 .

QD4:

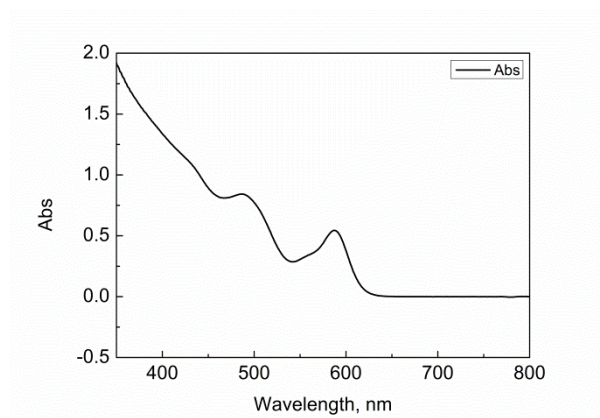


Figure S11. Absorption spectrum of QD4 in CHCl_3 .

QD5:

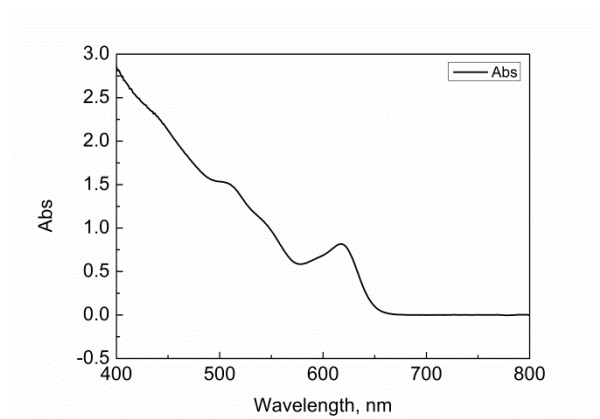


Figure S12. Absorption spectrum of QD5 in CHCl_3 .

Absorption spectra of QD:Pc:

QD1:

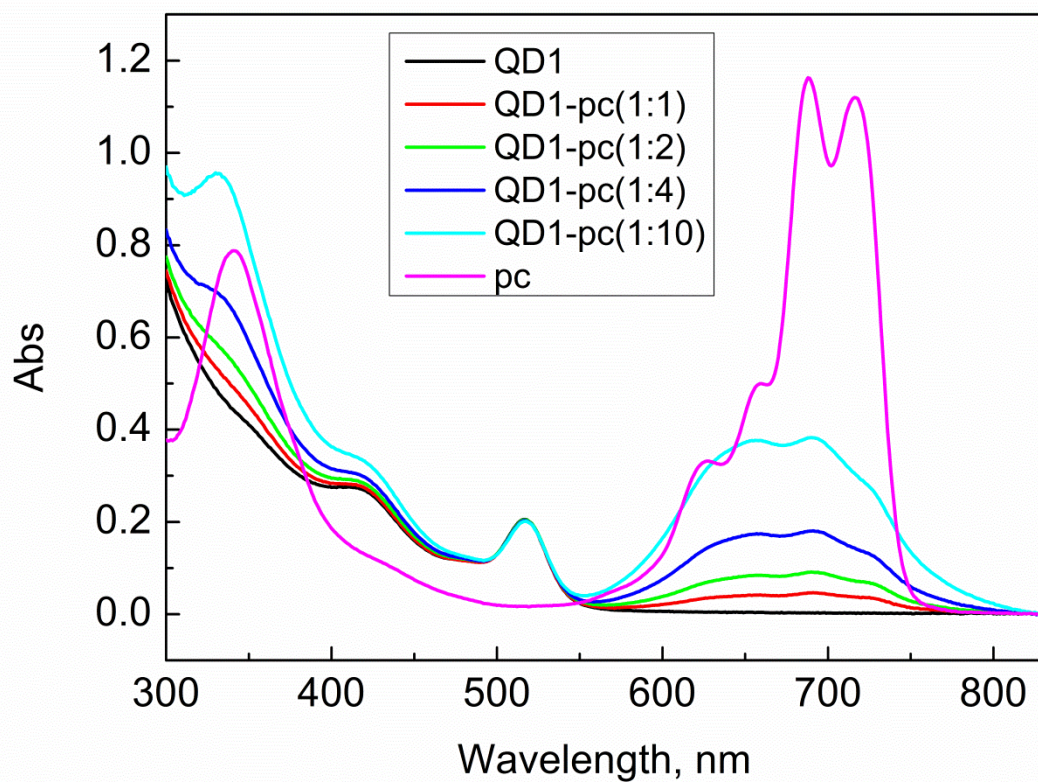


Figure S13. Absorption spectra of QD1, Pc and QD:Pc hybrids with different amounts of Pc in solution in CHCl₃.

QD3:

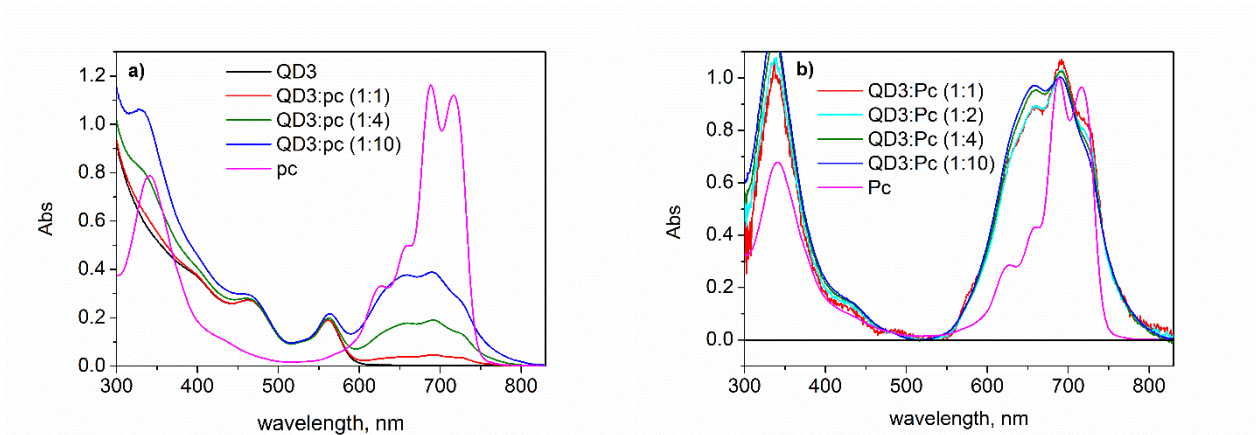


Figure S14. Left: absorption spectra of QD3, Pc and QD-Pc hybrids at different concentrations of Pc in CHCl_3 solution. Right: normalized absorption spectra of Pc in the QD-Pc hybrids at different relative concentrations of Pc obtained by subtracting the spectrum of QDs from that of the complex.

QD4:

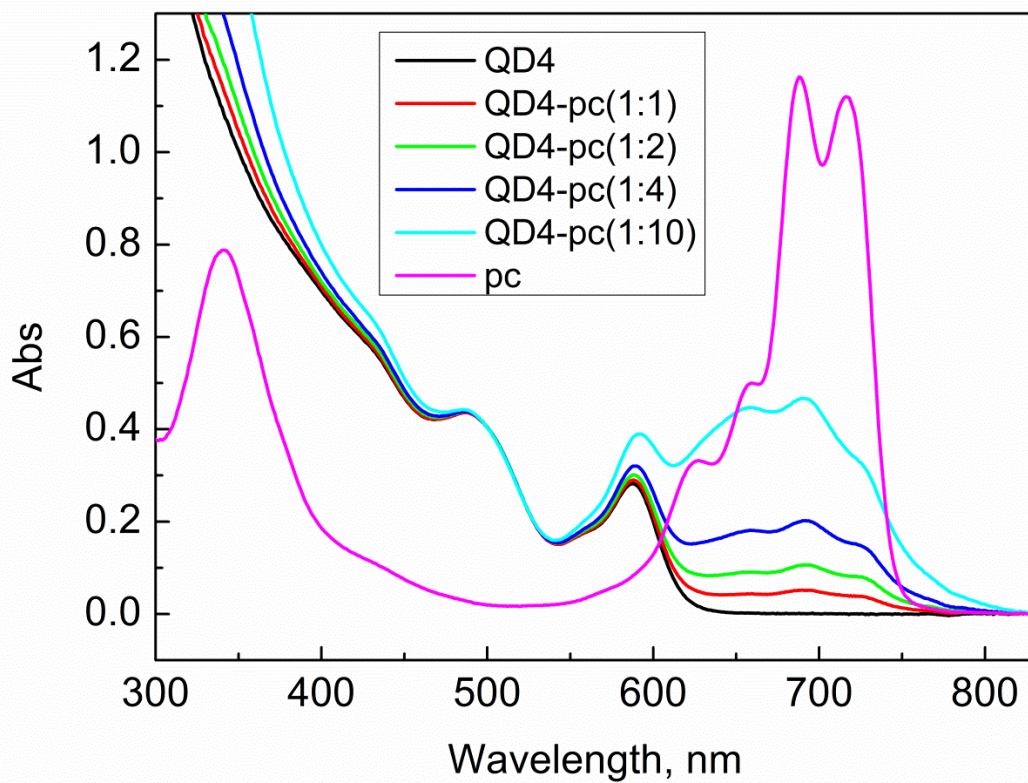


Figure S15. Absorption spectra of QD4, Pc and QD:Pc hybrids with different amounts of Pc in solution in CHCl_3 .

QD5:

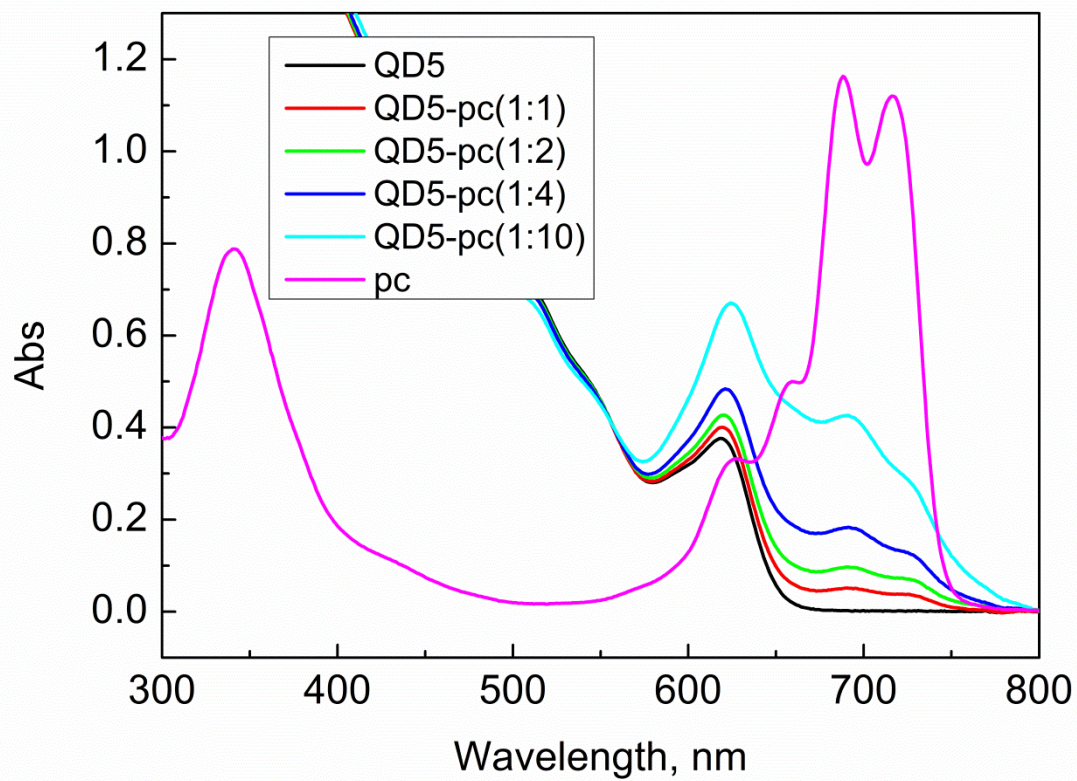


Figure S16. Absorption spectra of QD5, Pc and QD:Pc hybrids with different amounts of Pc in solution in CHCl_3 .

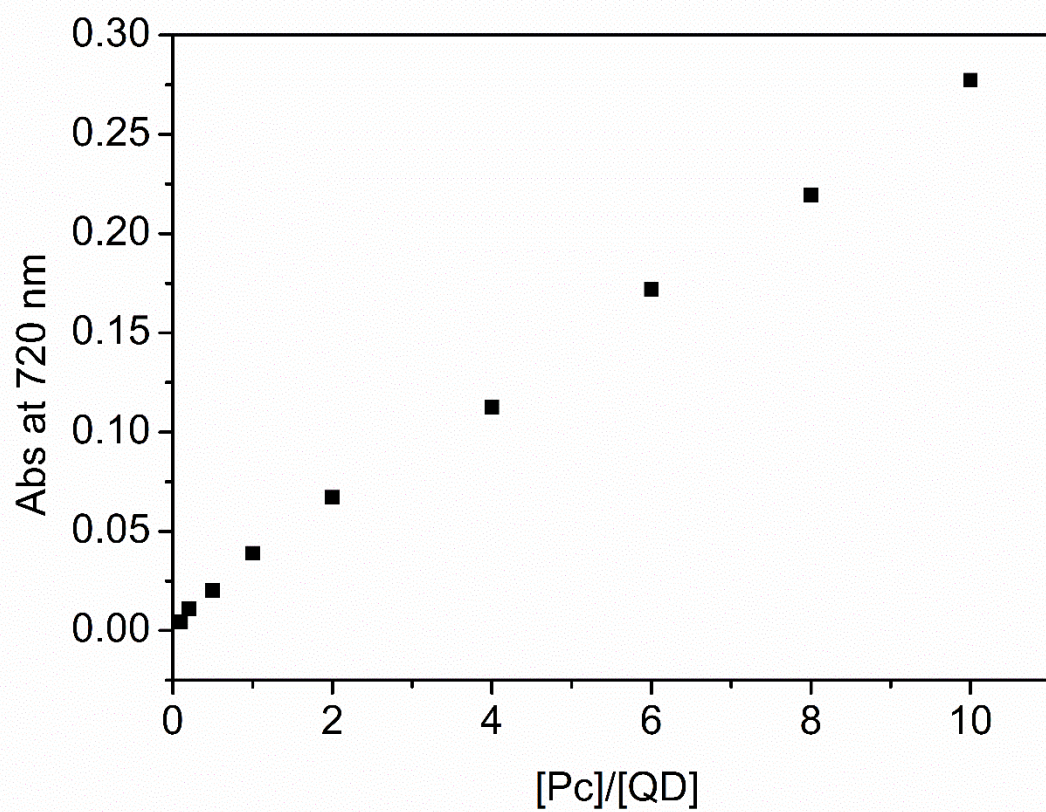


Figure S17. Absorption of QD2:Pc hybrids at 720 nm as a function of relative concentration of Pc.

Emission spectra of QDs and Pc:

QD1:Pc:

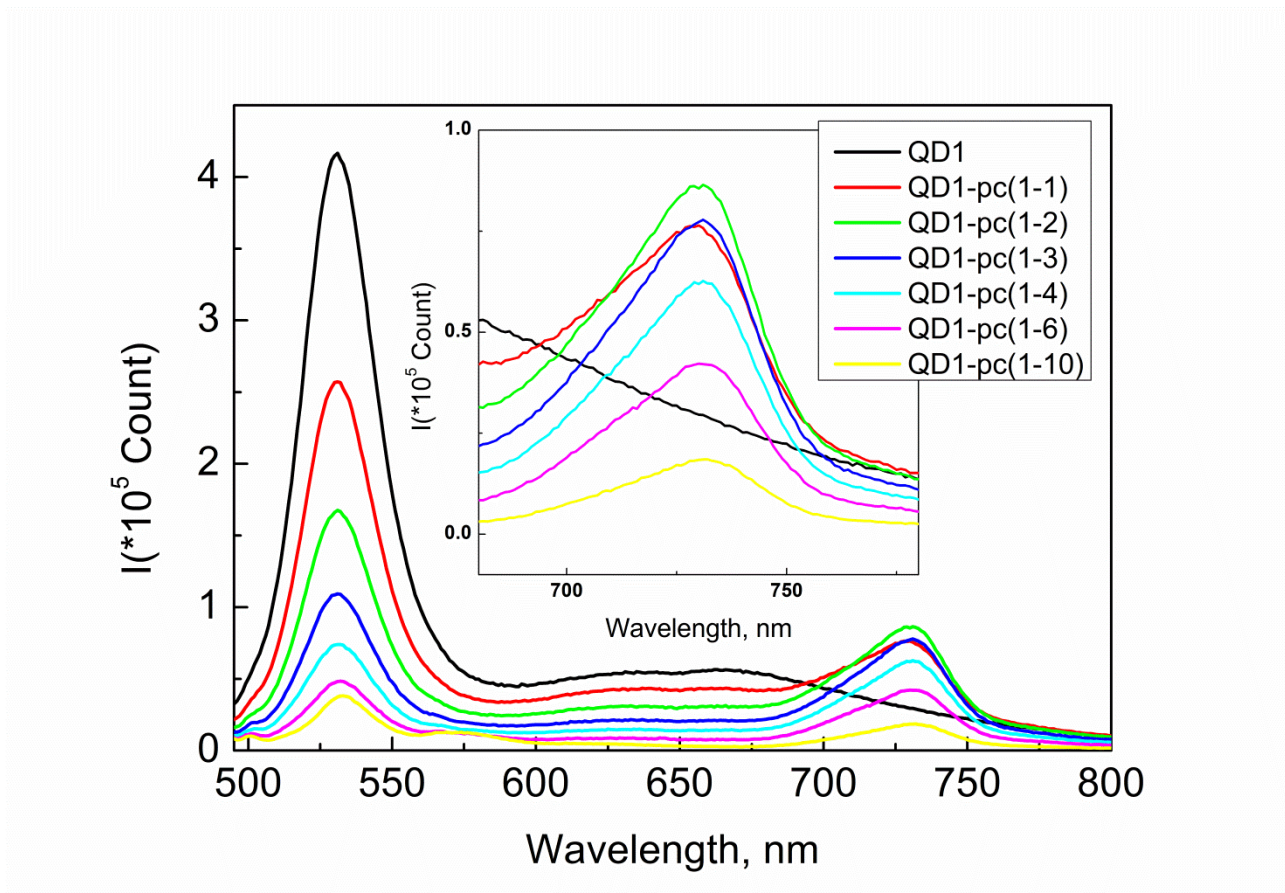


Figure S18. Emission spectra of QD1 only and QD1:Pc hybrids with different amounts of Pc in solution in chloroform when excited at 483 nm.

QD2:Pc:

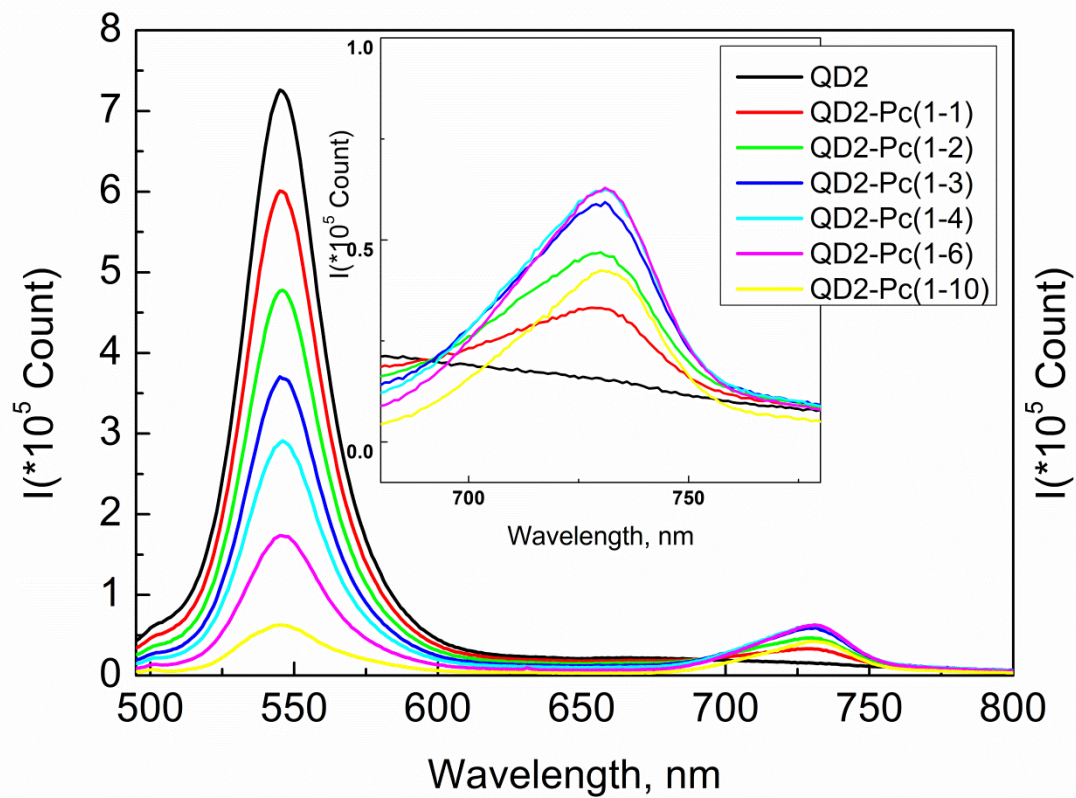


Figure S19. Emission spectra of QD2 only and QD2:Pc hybrids with different amounts of Pc in solution in chloroform when excited at 483 nm.

QD4:Pc:

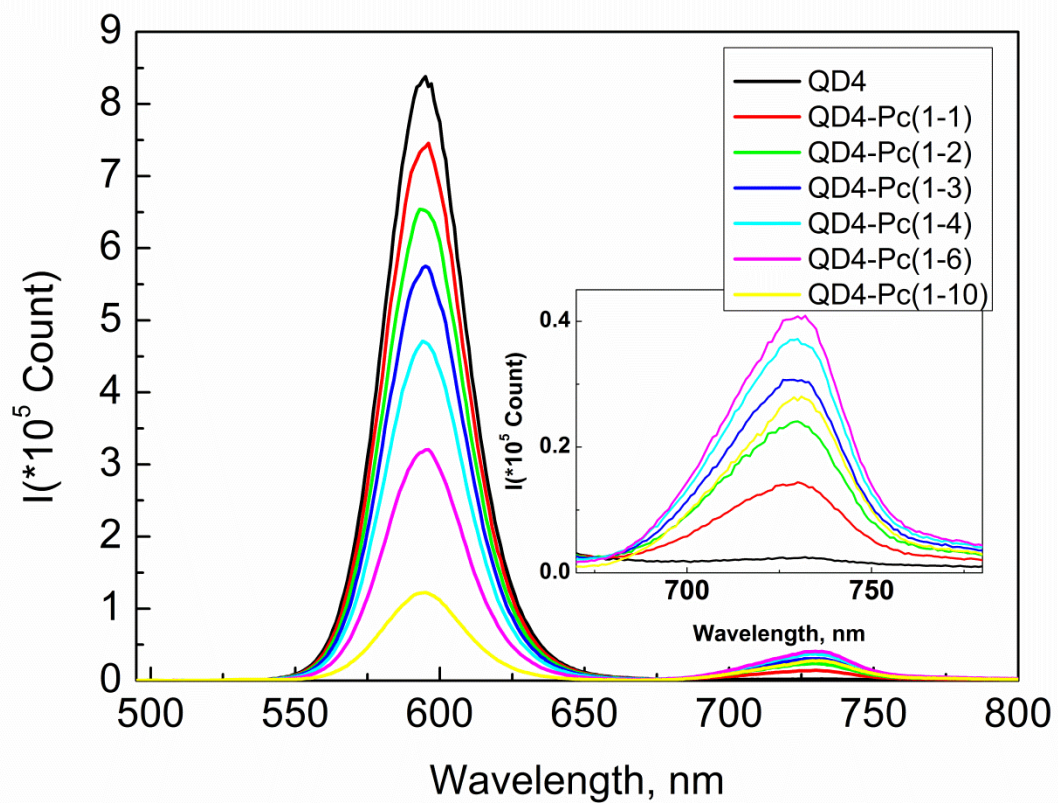


Figure S20. Emission spectra of QD4 only and QD4:Pc hybrids with different amounts of Pc in solution in chloroform when excited at 483 nm.

QD5:Pc:

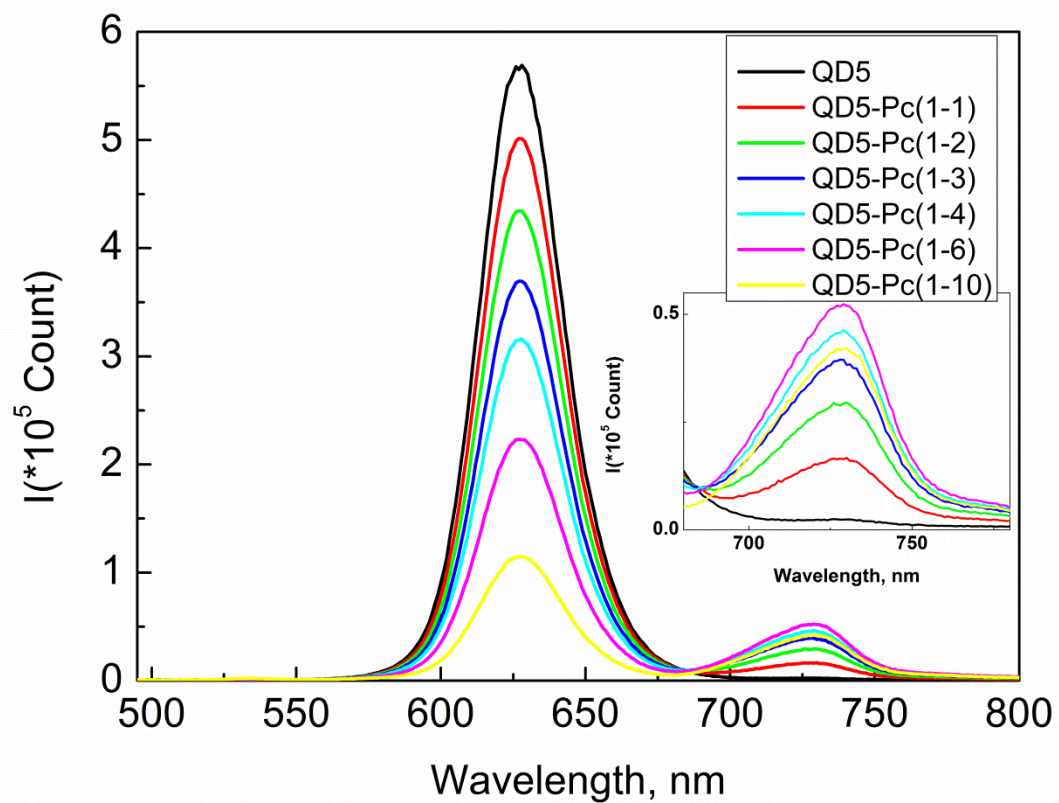


Figure S21. Emission spectra of QD5 only and QD5:Pc hybrids with different amounts of Pc in solution in chloroform when excited at 483 nm.

Emission of QDs and absorption of Pc:

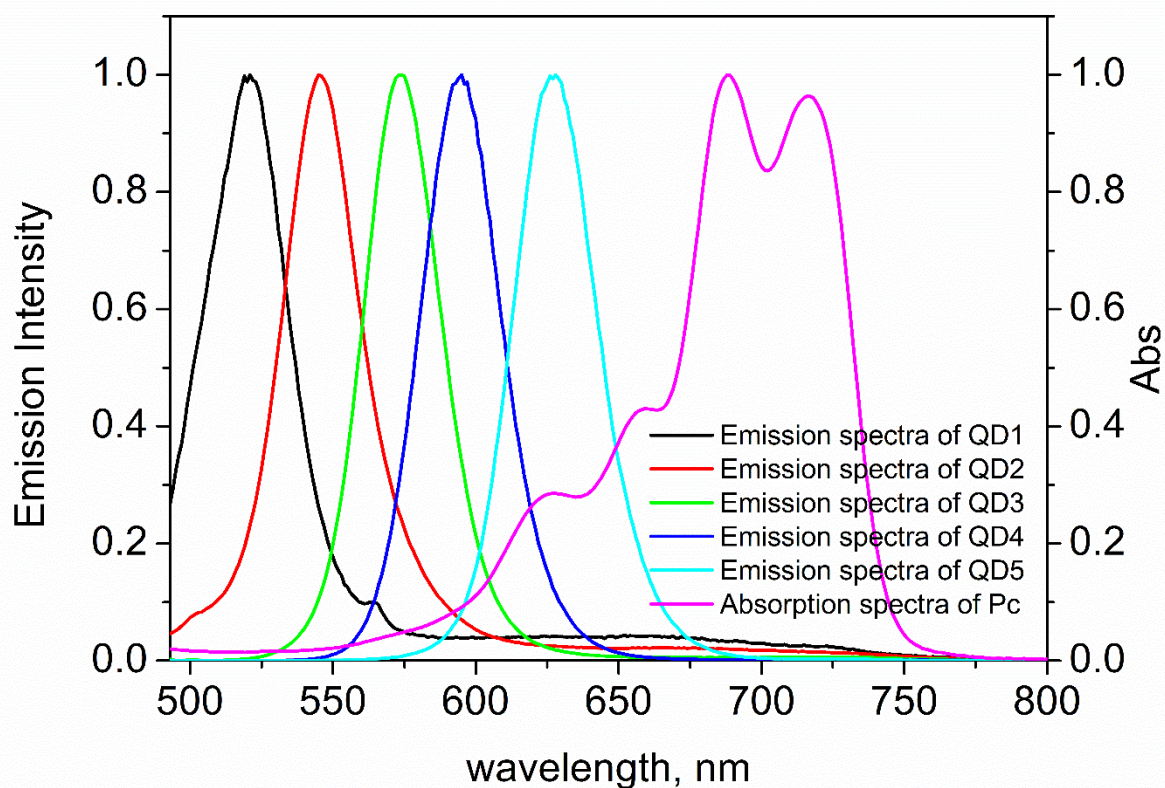


Figure S22. Normalized emission spectra of the QDs and normalized absorption spectrum of Pc used to calculate overlap integral.

The overlap integral measures the overlap between the emission spectrum of the QDs and absorption spectrum of Pc. The overlap integral is calculated numerically using Origin 8 software based on the following equation:

$$J = \int_0^{\infty} I(\lambda)\varepsilon_A(\lambda)\lambda^4 d\lambda$$

where $I(\lambda)$ is the emission spectrum of the QD normalized so that $\int_0^{\infty} I(\lambda)d\lambda = 1$, and $\varepsilon_A(\lambda)$ is the molar absorption of Pc. An absolute value for the molar absorption of Pc is not needed since our aim is to calculate the relative values of the overlap integral for different QDs with the same Pc.

Time Correlated Single Photon Counting (TCSPC):

QD1:Pc:

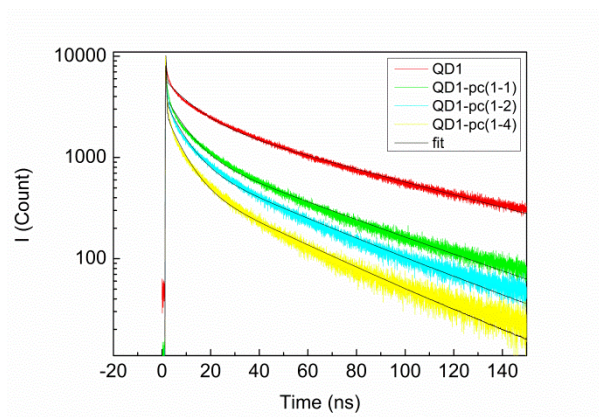


Figure S23. Fluorescence decay of QD1:Pc in CHCl_3 excited at 483 nm and monitored at 600 nm with the TCSPC method.

QD2:Pc:

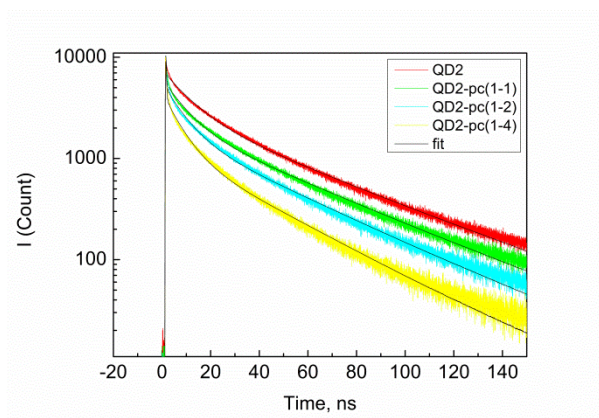


Figure S24. Fluorescence decay of QD2:Pc in CHCl_3 excited at 483 nm and monitored at 600 nm with the TCSPC method.

QD4:Pc:

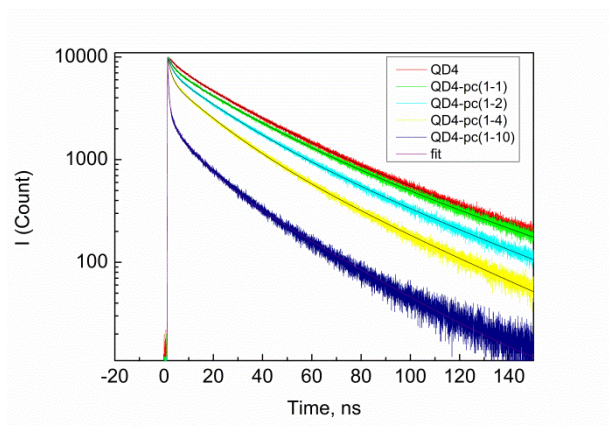


Figure S25. Fluorescence decay of QD4:Pc in CHCl_3 excited at 483 nm and monitored at 600 nm with the TCSPC method.

QD5:Pc:

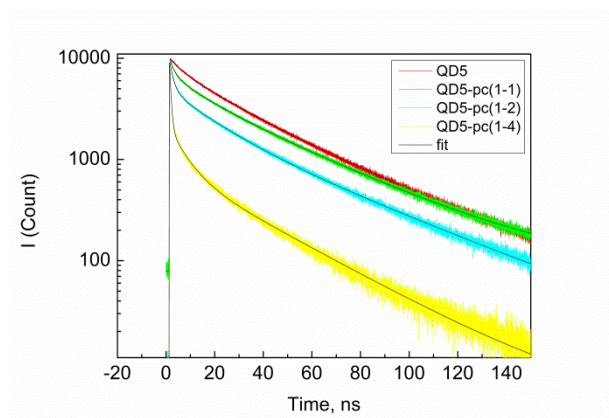


Figure S26. Fluorescence decay of QD5:Pc in CHCl_3 excited at 483 nm and monitored at 600 nm with the TCSPC method.

Transient absorption spectra of QD:Pc hybrids:

QD1:Pc hybrids:

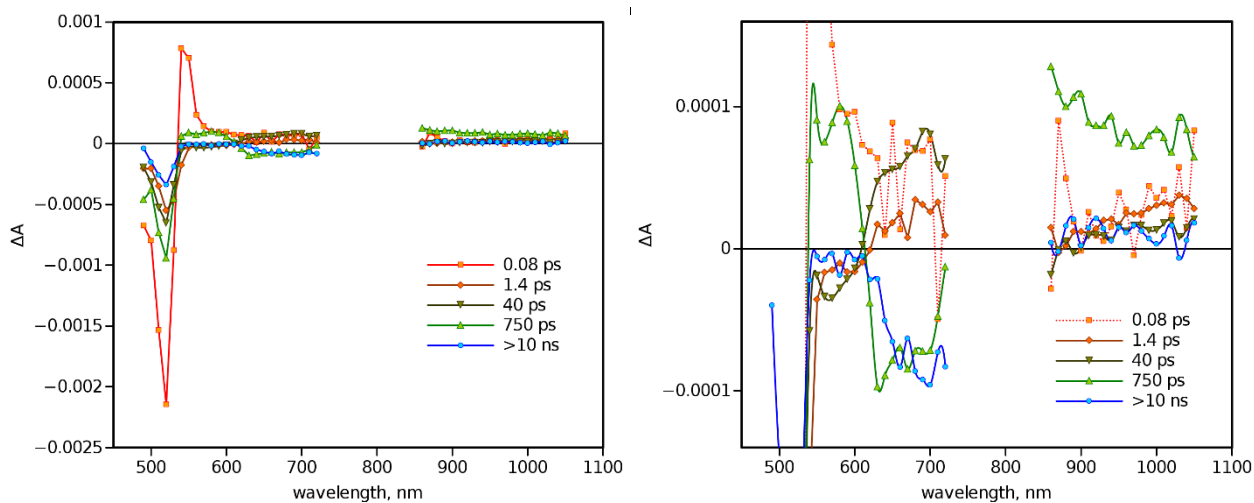


Figure S27. Left: transient absorption decay component spectra of QD1:Pc (1:7) in CHCl_3 after being excited at 480nm. Right: the same data but with an expended absorbance axis. The component time constant is indicated in the plots.

QD2:Pc hybrids:

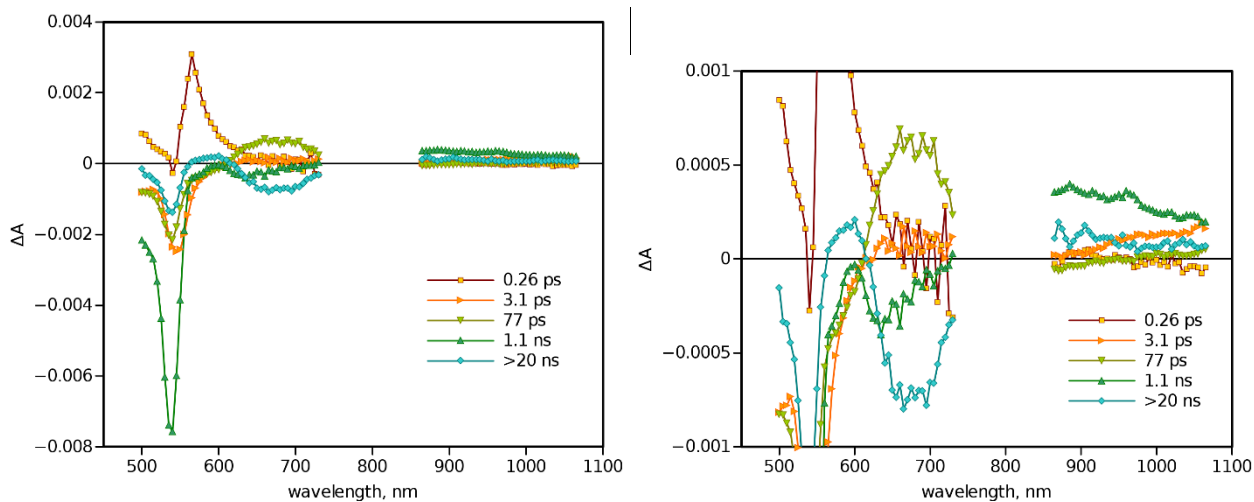


Figure S28. Left: transient absorption decay component spectra of QD2:Pc (1:7) in CHCl_3 after being excited at 480nm. Right: the same data but with an expended absorbance axis. The component time constant is indicated in the plots.

QD3:Pc hybrids:

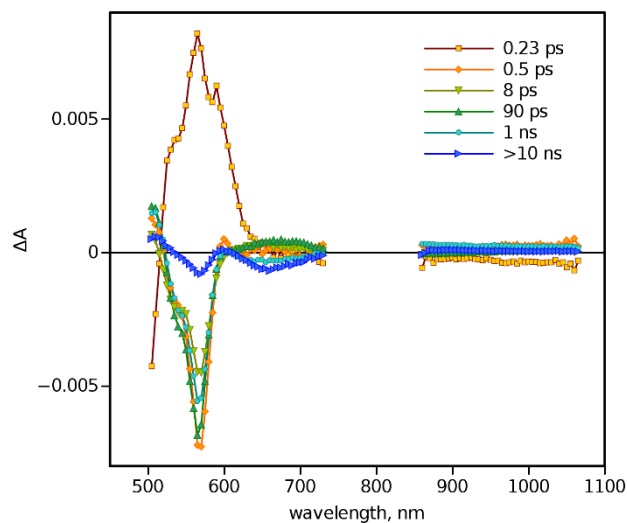


Figure S29. Transient absorption decay component spectra of QD3:Pc (1:7) in CHCl₃ after being excited at 480 nm .

QD4:Pc hybrids:

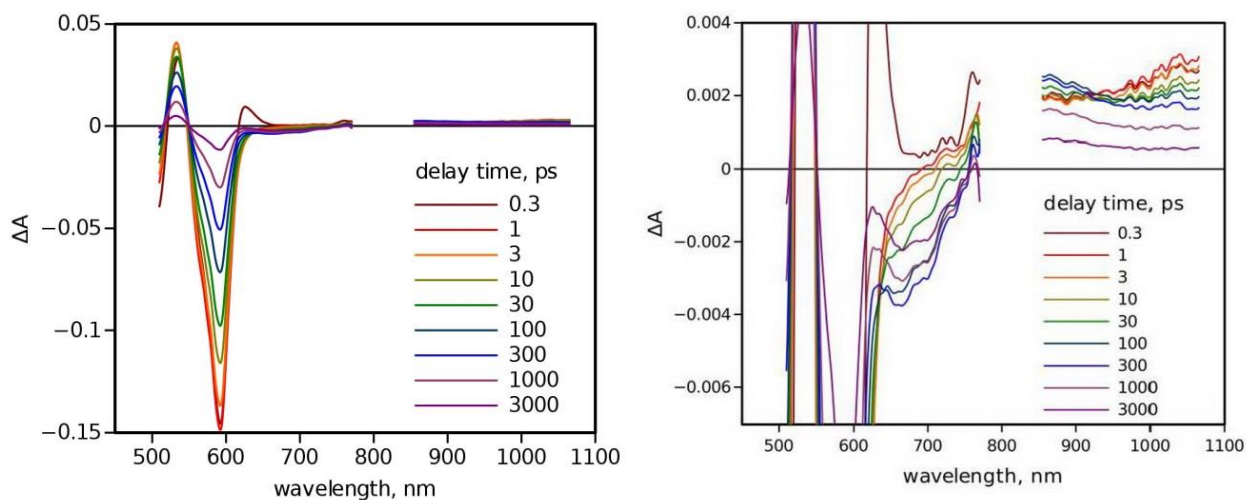


Figure S30. Time resolved transient absorption spectra of QD4:Pc (1:7) at selected delay times indicated in the plot in two different scales. Excitation wavelength is 480 nm.

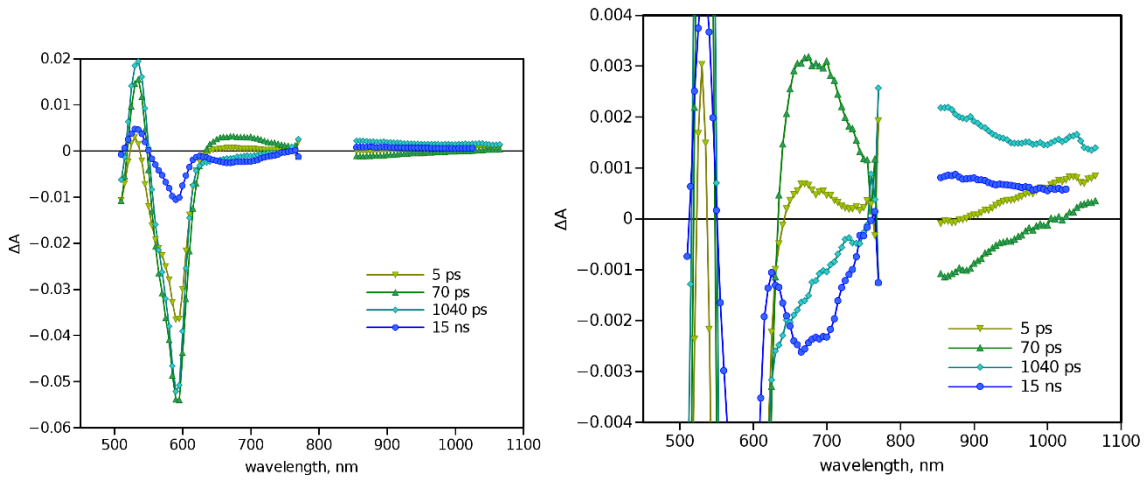


Figure S31. Decay component spectra of QD4:Pc sample. The plot on the right presents the same with expended absorption scale to show response in the red and NIR part of the spectrum. Excitation wavelength was 480 nm. The fast sub-picosecond response was ignored.

QD5:Pc hybrids

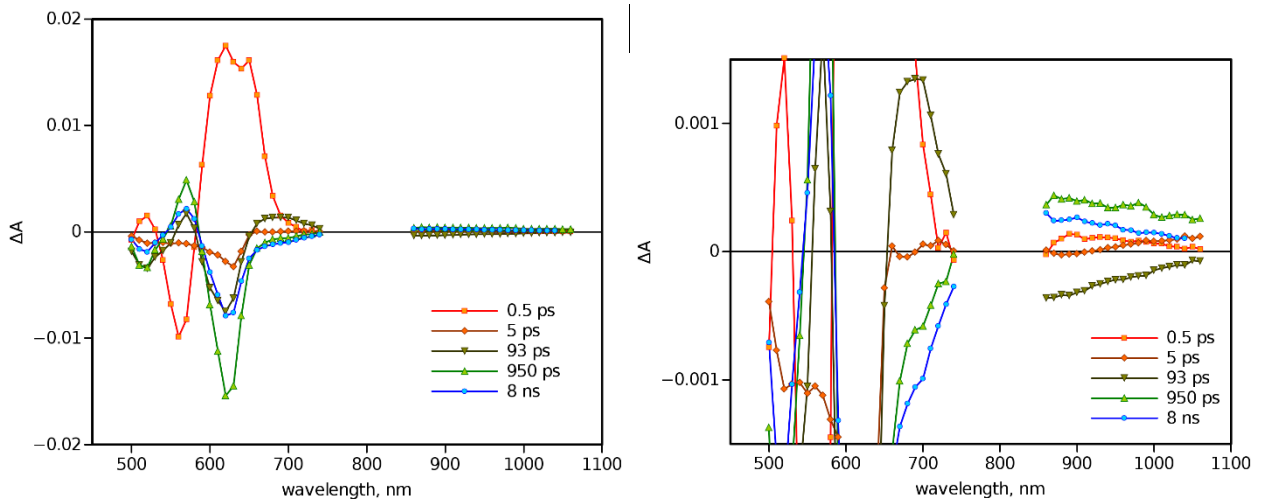


Figure S32. Left: transient absorption decay component spectra QD5:Pc (1:7) hybrid. Right: the same data but with expended absorbance axis.

References:

- [1] Vivo, Paola; Ojala, Mikko; Chukharev, Vladimir; Efimov, Alexander; Lemmetyinen, Helge. *J. Photochem. Photobiol. A Chemistry* 2009, 203 (2-3), 125-130